Supporting information on:

Tautomer identification troubles: The molecular structure of itaconic and citraconic anhydride revealed by rotational spectroscopy

Alexander Kanzow[a], Beppo Hartwig[a], Philipp Buschmann[b], Kevin G. Lengsfeld[b], Cara M. Höhne[b], Joshua S. Hoke[‡a], Finn Knüppe[‡a], Finn Köster[‡a], Jakob K. van Spronsen[‡a], Jens-Uwe Grabow[b], Don McNaughton[c] and Daniel A. Obenchain[*a]

a Institut für Physikalische Chemie, Georg-August-Universität Göttingen, Tammannstr. 6, 37077 Göttingen, Germany. E-mail: daniel.obenchain@uni-goettingen.de

b Institut für Physikalische Chemie and Elektrochemie, Gottfried Wilhelm Leibniz Universität, Callinstraße 3A, 30167 Hannover, Germany.

c School of Chemistry, Monash University, Wellington Road, 3800 Clayton, Australia.

‡ *These authors contributed equally to this work.*

Contents

In addition to the material provided here, the raw microwave spectra[1], all computational outputs[2] as well as the outputs of the experimental and structure fits[3] are provided on the GRO.data repository platform. All datasets can be centrally accessed at `https://data.goettingen-research-online.de/dataverse/ESI_Citraocnic_Itaconic_Microwave`.

1 Molecular structures

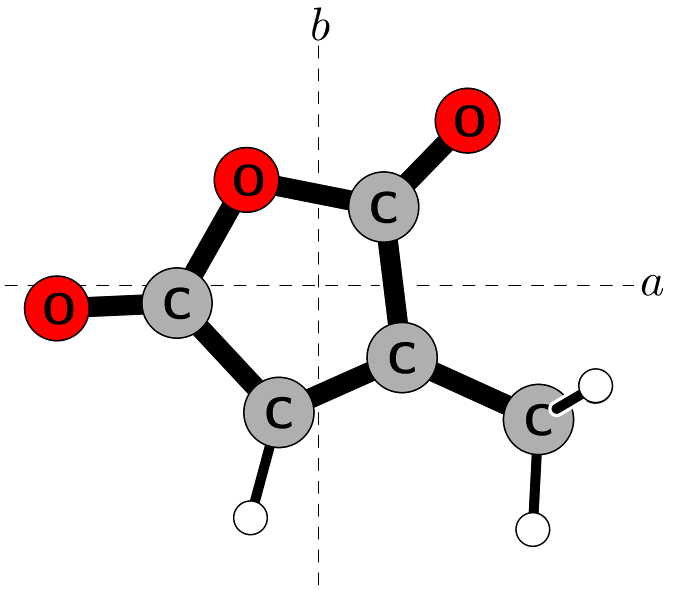

Fig. S1: Projections to the a,b-plane of the parent species of citraconic (left) and itaconic anhydride (right). The structures have been computed at the B3LYP level of theory.

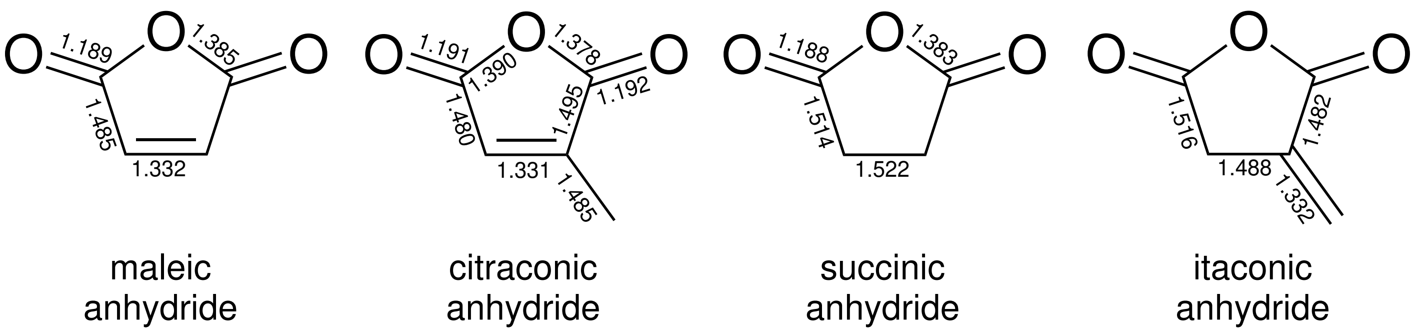

Fig. S2: Comparison of the semi-experimental equilibrium ($r^{\mathrm{SE}}_{0\rightarrow\mathrm{e}}$) bond distances of maleic anhydride[4], citraconic anhydride (CA), succinic anhydride[5] and itaconic anhydride (IA). The vibrational corrections have been obtained at the MP2/aVTZ and B3LYP/VTZ level of theory for maleic anhydride and succinic anhydride, respectively. The values shown for CA and IA have been obtained with DSD-PBEP86-D3(BJ)/aVTZ and correspond to those shown in Fig. 9 of the main text. Similar values to those of DSD-PBEP86-D3(BJ)/aVTZ have been obtained with MP2/aVTZ and B3LYP-D3(BJ)/aVTZ (see Tabs. S5 and S7) warranting this comparison. All distances are given in Å.

2 Rotational constants and predictions

Tab. S1: Comparison of the experimental results of citraconic anhydride with the theoretical predictions. All predicted values are equilibrium ones. κ refers to Ray's asymmetry parameter, N to the number of lines and σ to the root mean square error of the fit. Values in brackets were kept fixed during the fit. Note that despite having a 0 dipole moment along the c-axis, c-type transitions can still be observed for the E state.

	Experiment	B3LYP	PBE0	CAM-B3LYP	LC-ωPBE
A / MHz	3914.012 07(26)	3919.2338	3955.5895	3949.6876	3962.2062
B / MHz	1886.045 890(82)	1891.6604	1906.0507	1906.7828	1911.3780
C / MHz	1282.788 828(67)	1285.8446	1296.4159	1296.1035	1299.6006
D_J / kHz	0.0543(12)	0.054 66	0.054 97	0.054 68	0.054 56
D_{JK} / kHz	0.0989(29)	0.1002	0.093 25	0.095	0.088 84
D_K / kHz	1.488(12)	1.447	1.509	1.478	1.514
d_1 / kHz	−0.019 52(21)	−0.019 59	−0.019 65	−0.019 57	−0.019 56
d_2 / kHz	−0.003 62(12)	−0.003 429	−0.003 280	−0.003 352	−0.003 248
F / GHz	[164.07]	-	-	-	-
V_3 / cm^{-1}	326.5153(61)	319.69	294.97	320.96	301.49
V_3 / kJ mol^{-1}	3.905 990(74)	3.8243	3.5287	3.8395	3.6066
ρ / °	1.307	-	-	-	-
β / °	12.06	-	-	-	-
$D_{\pi 2J}$ / MHz	0.009 89(87)	-	-	-	-
$D_{\pi 2K}$ / MHz	−0.1155(29)	-	-	-	-
δ / °	23.909(92)	-	-	-	-
$\|\mu_a\|$ / Debye	strong	2.66	2.66	2.67	2.62
$\|\mu_b\|$ / Debye	very strong	4.03	3.97	4.05	3.98
$\|\mu_c\|$ / Debye	none	0	0	0	0
κ	−0.541 46	−0.539 90	−0.541 49	−0.539 73	−0.540 47
N	97	-	-	-	-
σ / kHz	1.56	-	-	-	-

	Experiment	M06-2X	B2PLYP	DSD-PBEP86	MP2
A / MHz	3914.012 07(26)	3964.9667	3921.3473	3927.6311	3928.0099
B / MHz	1886.045 890(82)	1901.4677	1887.8959	1888.2051	1883.6640
C / MHz	1282.788 828(67)	1295.3045	1284.3363	1285.2118	1283.1189
D_J / kHz	0.0543(12)	0.054 56	0.055 05	0.054 92	0.055 34
D_{JK} / kHz	0.0989(29)	0.092 17	0.097 66	0.092 49	0.091 85
D_K / kHz	1.488(12)	1.537	1.475	1.504	1.527
d_1 / kHz	−0.019 52(21)	−0.019 43	−0.019 66	−0.019 60	−0.019 71
d_2 / kHz	−0.003 62(12)	−0.003 297	−0.003 407	−0.003 333	−0.003 347
F / GHz	[164.07]	-	-	-	-
V_3 / cm^{-1}	326.5153(61)	328.49	326.01	326.58	330.57
V_3 / kJ mol^{-1}	3.905 990(74)	3.9296	3.8999	3.9067	3.9545
ρ / °	1.307	-	-	-	-
β / °	12.06	-	-	-	-
$D_{\pi 2J}$ / MHz	0.009 89(87)	-	-	-	-
$D_{\pi 2K}$ / MHz	−0.1155(29)	-	-	-	-
δ / °	23.909(92)	-	-	-	-
$\|\mu_a\|$ / Debye	strong	2.66	2.61	2.58	2.52

$\|\mu_b\|$ / Debye	very strong	4.03	4.03	3.99	3.98
$\|\mu_c\|$ / Debye	none	0	0	0	0
κ	−0.541 46	−0.545 89	−0.542 24	−0.543 61	−0.545 88
N	97	-	-	-	-
σ / kHz	1.56	-	-	-	-

Tab. S2: Rotational constants of the mono-substituted ^{13}C and ^{18}O isotopologues of citraconic anhydride. Centrifugal distortion parameters of all species were fixed to the values of the parent species (see Tab. S1).

Species	A / MHz	B / MHz	C / MHz	N	σ / kHz
$^{13}C_1$	3913.165 90(48)	1872.505 39(32)	1276.420 00(13)	16	2.10
$^{13}C_3$	3896.487 86(35)	1883.221 39(24)	1279.596 22(11)	12	1.54
$^{13}C_4$	3899.079 76(23)	1881.279 35(16)	1278.981 152(62)	16	1.02
$^{13}C_5$	3866.578 85(69)	1885.014 59(27)	1277.182 75(11)	14	1.71
$^{13}C_9$	3864.185 90(60)	1852.790 83(24)	1262.040 627(95)	14	1.56
$^{18}O_2$	3850.6761(12)	1878.9113(11)	1272.649 31(45)	8	3.90
$^{18}O_7$	3911.094 80(70)	1797.403 88(65)	1240.863 18(30)	8	2.52
$^{18}O_8$	3766.3001(20)	1855.4608(19)	1252.632 82(74)	8	6.48

Tab. S3: Comparison of the experimental results of itaconic anhydride with the theoretical predictions. All predicted values are equilibrium ones. κ refers to Ray's asymmetry parameter, N to the number of lines and σ to the root mean square error of the fit.

	Experiment	B3LYP	PBE0	CAM-B3LYP	LC-ωPBE
A / MHz	3901.067 97(19)	3883.406	3920.296	3917.678	3933.013
B / MHz	1921.856 99(17)	1914.358	1930.353	1931.359	1938.465
C / MHz	1298.788 83(12)	1293.251	1304.666	1304.79	1309.809
D_J / kHz	0.0573(21)	0.053 03	0.052 83	0.052 58	0.052 17
D_{JK} / kHz	0.1212(55)	0.1128	0.1061	0.1081	0.1029
D_K / kHz	1.040(11)	0.9998	1.049	1.022	1.047
d_1 / kHz	−0.0208(12)	−0.019 64	−0.019 58	−0.019 46	−0.019 37
d_2 / kHz	−0.003 93(44)	−0.004 093	−0.003 997	−0.004 014	−0.003 940
$\|\mu_a\|$ / Debye	strong	1.97	1.93	1.98	1.93
$\|\mu_b\|$ / Debye	strong	4.58	4.52	4.63	4.55
$\|\mu_c\|$ / Debye	none	0	0	0	0
κ	−0.521 14	−0.522 49	−0.523 78	−0.522 64	−0.523 01
N	46	-	-	-	-
σ / kHz	1.39	-	-	-	-
	Experiment	M06-2X	B2PLYP	DSD-PBEP86	MP2
A / MHz	3901.067 97(19)	3950.755	3914.538	3917.282	3915.847
B / MHz	1921.856 99(17)	1938.109	1921.377	1923.36	1918.649
C / MHz	1298.788 83(12)	1310.784	1299.115	1300.393	1298.066
D_J / kHz	0.0573(21)	0.052 25	0.053 32	0.053 04	0.053 49
D_{JK} / kHz	0.1212(55)	0.1036	0.1113	0.107	0.1069
D_K / kHz	1.040(11)	1.055	1.015	1.03	1.069
d_1 / kHz	−0.0208(12)	−0.019 31	−0.019 66	−0.019 55	−0.019 65

d_2 / kHz	$-0.003\,93(44)$	$-0.003\,938$	$-0.004\,042$	$-0.003\,961$	$-0.003\,927$
$\|\mu_a\|$ / Debye	strong	1.96	1.94	1.91	1.84
$\|\mu_b\|$ / Debye	strong	4.6	4.55	4.5	4.44
$\|\mu_c\|$ / Debye	none	0	0	0	0
κ	$-0.521\,14$	$-0.524\,75$	$-0.524\,16$	$-0.523\,89$	$-0.525\,87$
N	46	-	-	-	-
σ / kHz	1.39	-	-	-	-

Tab. S4: Rotational constants of the mono-substituted ^{13}C isotopologues of itaconic anhydride. Centrifugal distortion parameters of all species were fixed to the values of the parent species (see Tab. S3).

Species	A / MHz	B / MHz	C / MHz	N	σ / kHz
$^{13}C_1$	3900.9192(60)	1907.9750(23)	1292.415 74(53)	8	1.29
$^{13}C_3$	3886.0263(60)	1917.7549(24)	1295.246 76(53)	8	0.58
$^{13}C_4$	3883.843(12)	1916.3125(49)	1294.3479(17)	8	0.46
$^{13}C_5$	3849.1270(62)	1919.9509(28)	1292.128 99(62)	7	0.92
$^{13}C_{10}$	3846.6294(57)	1891.1040(23)	1278.709 01(50)	8	1.15

3 Structure determination

3.1 r_S and $r_{0\rightarrow e}^{SE}$ results

Tab. S5: Overview of bond distances (d) and angles ($\angle$) obtained with Kraitchman's substitution method (r_S) and semi-experimental equilibrium structure ($r_{0\rightarrow e}^{SE}$) fits where only the underlying computational method is specified of citraconic anhydride (CA). Values in brackets were derived and not fit, which is typical of fitting ring structures. σ refers to the uncertainty of the respective structure fit.

	r_S	B3LYP	PBE0	CAM-B3LYP	LC-ωPBE
$d(C_1\text{-}O_7)$ / Å	1.196(19)	1.1908(25)	1.1913(21)	1.1905(28)	1.1898(15)
$d(C_1\text{-}O_2)$ / Å	1.390(10)	1.393(12)	1.3929(99)	1.388(14)	1.3866(70)
$d(C_3\text{-}O_2)$ / Å	1.3755(32)	1.3787(57)	1.3799(48)	1.3800(65)	1.3786(34)
$d(C_3\text{-}O_8)$ / Å	1.2022(51)	1.1870(36)	1.1888(31)	1.1895(41)	1.1896(22)
$d(C_3\text{-}C_4)$ / Å	1.484 22(29)	1.4983(60)	1.4975(51)	1.4950(69)	1.4950(36)
$d(C_4\text{-}C_9)$ / Å	1.491 99(8)	1.4805(40)	1.4835(34)	1.4819(45)	1.4819(24)
$d(C_4\text{-}C_5)$ / Å	1.327 47(51)	1.3379(71)	1.3344(60)	1.3370(81)	1.3376(42)
$d(C_1\text{-}C_5)$ / Å	1.4920(11)	[1.470(11)]	[1.4698(89)]	[1.479(12)]	[1.4835(63)]
$\angle(O_7\text{-}C_1\text{-}O_2)$ / °	122.42(70)	121.7(1.2)	121.7(1.0)	122.2(1.4)	122.54(74)
$\angle(O_7\text{-}C_1\text{-}C_5)$ / °	129.86(75)	[130.4(1.1)]	[130.34(90)]	[129.9(1.2)]	[129.60(63)]
$\angle(C_5\text{-}C_1\text{-}O_2)$ / °	107.72(17)	[107.92(26)]	[107.92(22)]	[107.98(29)]	[107.86(15)]
$\angle(C_1\text{-}O_2\text{-}C_3)$ / °	107.82(25)	108.15(32)	108.07(28)	108.19(37)	108.29(20)
$\angle(O_2\text{-}C_3\text{-}O_8)$ / °	122.45(19)	123.08(43)	122.96(36)	122.94(49)	123.05(26)
$\angle(O_2\text{-}C_3\text{-}C_4)$ / °	108.96(20)	108.35(34)	108.29(29)	108.39(39)	108.52(21)
$\angle(O_8\text{-}C_3\text{-}C_4)$ / °	128.59(21)	[128.57(44)]	[128.74(37)]	[128.67(50)]	[128.43(26)]
$\angle(C_3\text{-}C_4\text{-}C_9)$ / °	121.49(17)	121.25(49)	121.09(42)	121.16(56)	121.41(30)
$\angle(C_3\text{-}C_4\text{-}C_5)$ / °	107.39(18)	106.63(36)	106.74(30)	106.94(41)	106.85(21)
$\angle(C_9\text{-}C_4\text{-}C_5)$ / °	131.12(20)	[132.12(43)]	[132.17(37)]	[131.89(50)]	[131.75(26)]
$\angle(C_4\text{-}C_5\text{-}C_1)$ / °	108.11(60)	[108.95(91)]	[108.98(77)]	[108.5(1.0)]	[108.48(54)]
σ / MHz	-	0.174	0.146	0.200	0.106

	r_S	M06-2X	B2PLYP	DSD-PBEP86	MP2
$d(C_1\text{-}O_7)$ / Å	1.196(19)	1.1916(35)	1.1910(22)	1.1905(60)	1.1907(7)
$d(C_1\text{-}O_2)$ / Å	1.390(10)	1.401(16)	1.384(10)	1.3897(30)	1.3939(31)
$d(C_3\text{-}O_2)$ / Å	1.3755(32)	1.3793(78)	1.3765(50)	1.3775(14)	1.3776(15)
$d(C_3\text{-}O_8)$ / Å	1.2022(51)	1.1883(50)	1.1907(32)	1.1916(9)	1.1892(10)
$d(C_3\text{-}C_4)$ / Å	1.484 22(29)	1.5007(82)	1.4955(53)	1.4951(15)	1.4949(16)
$d(C_4\text{-}C_9)$ / Å	1.491 99(8)	1.4836(55)	1.4825(35)	1.4845(10)	1.4821(11)
$d(C_4\text{-}C_5)$ / Å	1.327 47(51)	1.3306(98)	1.3343(62)	1.3310(18)	1.3358(19)
$d(C_1\text{-}C_5)$ / Å	1.4920(11)	[1.467(14)]	[1.4839(92)]	[1.4802(26)]	[1.4756(27)]
$\angle(O_7\text{-}C_1\text{-}O_2)$ / °	122.42(70)	120.9(1.7)	122.5(1.1)	121.84(31)	121.27(32)
$\angle(O_7\text{-}C_1\text{-}C_5)$ / °	129.86(75)	[131.3(1.5)]	[129.60(93)]	[130.28(27)]	[130.83(28)]
$\angle(C_5\text{-}C_1\text{-}O_2)$ / °	107.72(17)	[107.85(35)]	[107.94(22)]	[107.88(7)]	[107.91(7)]
$\angle(C_1\text{-}O_2\text{-}C_3)$ / °	107.82(25)	107.87(44)	108.29(29)	108.12(8)	108.11(9)
$\angle(O_2\text{-}C_3\text{-}O_8)$ / °	122.45(19)	122.97(58)	123.24(38)	123.13(11)	123.44(11)
$\angle(O_2\text{-}C_3\text{-}C_4)$ / °	108.96(20)	108.26(47)	108.48(30)	108.40(9)	108.39(9)
$\angle(O_8\text{-}C_3\text{-}C_4)$ / °	128.59(21)	[128.77(60)]	[128.28(39)]	[128.47(11)]	[128.16(12)]
$\angle(C_3\text{-}C_4\text{-}C_9)$ / °	121.49(17)	120.70(67)	121.39(47)	121.12(13)	121.50(13)
$\angle(C_3\text{-}C_4\text{-}C_5)$ / °	107.39(18)	106.81(49)	106.90(32)	107.06(9)	107.01(10)
$\angle(C_9\text{-}C_4\text{-}C_5)$ / °	131.12(20)	[132.49(59)]	[131.71(38)]	[131.82(11)]	[131.49(12)]

$\angle(\mathrm{C_4\text{-}C_5\text{-}C_1})$ / °	108.11(60)	[109.2(1.3)]	[108.39(80)]	[108.54(23)]	[108.58(24)]
σ / MHz	-	0.129	0.158	0.042	0.049

Tab. S6: Overview of bond distances (d) and angles ($\angle$) obtained with Kraitchman's substitution method (r_S), semi-experimental equilibrium structure ($r^\mathsf{SE}_{0\to\mathrm{e}}$) fits at the DSD-PBEP86 level of theory and equilibrium structures r_e at the DCSD-F12, CCSD(T)-F12c and AE-CCSD(T)-F12c (AE = all electron) level of theory of citraconic anhydride (CA). Values in brackets where derived and not fit. σ refers to the uncertainty of the respective structure fit.

	r_S	DSD-PBEP86	DCSD-F12b	CCSD(T)-F12c	AE-CCSD(T)-F12c
$d(\mathrm{C_1\text{-}O_7})$ / Å	1.196(19)	1.1905(60)	1.190 47	1.191 58	1.191 91
$d(\mathrm{C_1\text{-}O_2})$ / Å	1.390(10)	1.3897(30)	1.389 86	1.392 14	1.393 37
$d(\mathrm{C_3\text{-}O_2})$ / Å	1.3755(32)	1.3775(14)	1.380 32	1.381 53	1.382 66
$d(\mathrm{C_3\text{-}O_8})$ / Å	1.2022(51)	1.1916(9)	1.191 76	1.192 97	1.193 35
$d(\mathrm{C_3\text{-}C_4})$ / Å	1.484 22(29)	1.4951(15)	1.496 97	1.497 90	1.498 56
$d(\mathrm{C_4\text{-}C_9})$ / Å	1.491 99(8)	1.4845(10)	1.486 57	1.486 56	1.486 76
$d(\mathrm{C_4\text{-}C_5})$ / Å	1.327 47(51)	1.3310(18)	1.336 64	1.338 05	1.337 82
$d(\mathrm{C_1\text{-}C_5})$ / Å	1.4920(11)	[1.4802(26)]	1.483 66	1.483 94	1.484 50
$\angle(\mathrm{O_7\text{-}C_1\text{-}O_2})$ / °	122.42(70)	121.84(31)	122.159	122.138	122.131
$\angle(\mathrm{O_7\text{-}C_1\text{-}C_5})$ / °	129.86(75)	[130.28(27)]	129.980	130.006	130.041
$\angle(\mathrm{C_5\text{-}C_1\text{-}O_2})$ / °	107.72(17)	[107.88(7)]	107.861	107.856	107.828
$\angle(\mathrm{C_1\text{-}O_2\text{-}C_3})$ / °	107.82(25)	108.12(8)	108.184	108.164	108.157
$\angle(\mathrm{O_2\text{-}C_3\text{-}O_8})$ / °	122.45(19)	123.13(11)	122.872	122.926	122.909
$\angle(\mathrm{O_2\text{-}C_3\text{-}C_4})$ / °	108.96(20)	108.40(9)	108.512	108.507	108.476
$\angle(\mathrm{O_8\text{-}C_3\text{-}C_4})$ / °	128.59(21)	[128.47(11)]	128.616	128.567	128.615
$\angle(\mathrm{C_3\text{-}C_4\text{-}C_9})$ / °	121.49(17)	121.12(13)	121.319	121.248	121.266
$\angle(\mathrm{C_3\text{-}C_4\text{-}C_5})$ / °	107.39(18)	107.06(9)	106.871	106.887	106.921
$\angle(\mathrm{C_9\text{-}C_4\text{-}C_5})$ / °	131.12(20)	[131.82(11)]	131.810	131.865	131.813
$\angle(\mathrm{C_4\text{-}C_5\text{-}C_1})$ / °	108.11(60)	[108.54(23)]	108.571	108.585	108.618
σ / MHz	-	0.042	-	-	-

Tab. S7: Overview of bond distances (d) and angles ($\angle$) obtained with Kraitchman's substitution method (r_S) and semi-experimental equilibrium structure ($r^\mathsf{SE}_{0\to\mathrm{e}}$) fits where only the underlying computational method is specified of itaconic anhydride (IA). Values in brackets where derived and not fit. σ refers to the uncertainty of the respective structure fit.

	r_S	B3LYP	PBE0	CAM-B3LYP	LC-ωPBE
$d(\mathrm{C_1\text{-}C_5})$ / Å	1.532(17)	1.510(13)	1.5111(93)	1.509(13)	1.5117(72)
$d(\mathrm{C_4\text{-}C_5})$ / Å	1.4907(34)	1.493(17)	1.499(13)	1.503(18)	1.5028(99)
$d(\mathrm{C_3\text{-}C_4})$ / Å	1.3376(47)	1.331(87)	1.3303(67)	1.3299(92)	1.3297(52)
$d(\mathrm{C_4\text{-}C_{10}})$/ Å	1.4789(29)	1.4843(93)	1.4871(72)	1.4890(99)	1.4910(56)
$\angle(\mathrm{C_1\text{-}C_5\text{-}C_4})$ / °	102.83(47)	103.35(48)	103.34(37)	103.37(50)	103.37(29)
$\angle(\mathrm{C_5\text{-}C_4\text{-}C_{10}})$ / °	130.27(18)	130.88(96)	130.94(74)	131.0(1.0)	131.03(58)
$\angle(\mathrm{C_5\text{-}C_4\text{-}C_3})$ / °	107.51(17)	107.48(59)	107.27(45)	107.22(62)	107.14(35)
σ / MHz	-	0.374	0.287	0.398	0.217
	r_S	M06-2X	B2PLYP	DSD-PBEP86	MP2

$d(C_1\text{-}C_5)$ / Å	1.532(17)	1.5119(54)	1.5142(61)	1.5163(36)	1.518(10)
$d(C_4\text{-}C_5)$ / Å	1.4907(34)	1.5010(75)	1.4878(84)	1.4876(50)	1.480(14)
$d(C_3\text{-}C_4)$ / Å	1.3376(47)	1.3301(39)	1.3314(44)	1.3317(26)	1.3329(73)
$d(C_4\text{-}C_{10})$/ Å	1.4789(29)	1.4917(42)	1.4812(47)	1.4818(28)	1.4813(78)
$\angle(C_1\text{-}C_5\text{-}C_4)$ / °	102.83(47)	103.35(22)	103.24(24)	103.21(14)	103.18(40)
$\angle(C_5\text{-}C_4\text{-}C_{10})$ / °	130.27(18)	131.11(43)	130.59(48)	130.58(29)	130.62(81)
$\angle(C_5\text{-}C_4\text{-}C_3)$ / °	107.51(17)	107.18(27)	107.66(30)	107.60(18)	107.80(50)
σ / MHz	-	0.164	0.212	0.107	0.308

Tab. S8: Overview of bond distances (d) and angles ($\angle$) obtained with Kraitchman's substitution method (r_S), semi-experimental equilibrium structure ($r_{0\rightarrow e}^{\mathsf{SE}}$) fits at the DSD-PBEP86 level of theory and equilibrium structures r_e at the DCSD-F12, CCSD(T)-F12c and AE-CCSD(T)-F12c (AE = all electron) level of theory of itaconic anhydride (IA). σ refers to the uncertainty of the respective structure fit.

	r_S	DSD-PBEP86	DCSD-F12b	CCSD(T)-F12c	AE-CCSD(T)-F12c
$d(C_1\text{-}C_5)$ / Å	1.532(17)	1.5163(36)	1.516 64	1.517 53	1.518 15
$d(C_4\text{-}C_5)$ / Å	1.4907(34)	1.4876(50)	1.498 61	1.498 73	1.499 26
$d(C_3\text{-}C_4)$ / Å	1.4789(29)	1.3317(26)	1.490 65	1.490 51	1.491 08
$d(C_4\text{-}C_{10})$ / Å	1.3376(47)	1.4818(28)	1.331 69	1.332 81	1.332 52
$\angle(C_1\text{-}C_5\text{-}C_4)$ / °	102.83(47)	103.21(14)	103.211	103.237	103.262
$\angle(C_5\text{-}C_4\text{-}C_{10})$ / °	130.27(18)	130.58(29)	130.779	130.853	130.783
$\angle(C_5\text{-}C_4\text{-}C_3)$ / °	107.51(17)	107.60(18)	107.280	107.369	107.373
σ / MHz	-	0.107	-	-	-

3.2 $r_m^{(1)}$ and $r_m^{(2)}$ results

Tab. S9: Overview of bond distances (d) and angles ($\angle$) obtained with Kraitchman's substitution method (r_S) and mass dependent $r_m^{(1)}$ structure fits where only the underlying computational method is specified of citraconic anhydride (CA). Values in brackets were derived and not fit and the given errors are unreliable. σ refers to the uncertainty of the respective structure fit.

	r_S	B3LYP	PBE0	CAM-B3LYP	LC-ωPBE
d(C$_1$-O$_7$) / Å	1.196(19)	1.193 73(64)	1.193 74(66)	1.193 70(63)	1.193 65(60)
d(C$_1$-O$_2$) / Å	1.390(10)	1.3898(31)	1.3899(31)	1.3897(30)	1.3897(29)
d(C$_3$-O$_2$) / Å	1.3755(32)	1.3723(27)	1.3723(28)	1.3723(26)	1.3723(25)
d(C$_3$-O$_8$) / Å	1.2022(51)	1.2007(11)	1.2008(11)	1.2006(11)	1.2007(10)
d(C$_3$-C$_4$) / Å	1.484 22(29)	1.4857(22)	1.4858(23)	1.4855(22)	1.4853(21)
d(C$_4$-C$_9$) / Å	1.491 99(8)	1.4903(10)	1.4904(11)	1.4903(10)	1.490 18(97)
d(C$_4$-C$_5$) / Å	1.327 47(51)	1.3300(32)	1.3299(33)	1.3299(31)	1.3294(30)
d(C$_1$-C$_5$) / Å	1.4920(11)	[1.4844(32)]	[1.4843(32)]	[1.4845(31)]	[1.4846(30)]
$\angle$(O$_7$-C$_1$-O$_2$) / °	122.42(70)	122.34(34)	122.32(35)	122.34(33)	122.32(32)
$\angle$(O$_7$-C$_1$-C$_5$) / °	129.86(75)	[129.78(30)]	[129.79(31)]	[129.77(29)]	[129.81(28)]
$\angle$(C$_5$-C$_1$-O$_2$) / °	107.72(17)	[107.88(11)]	[107.89(11)]	[107.88(11)]	[107.87(10)]
$\angle$(C$_1$-O$_2$-C$_3$) / °	107.82(25)	107.824(93)	107.818(95)	107.823(91)	107.813(87)
$\angle$(O$_2$-C$_3$-O$_8$) / °	122.45(19)	122.64(12)	122.64(12)	122.63(11)	122.62(11)
$\angle$(O$_2$-C$_3$-C$_4$) / °	108.96(20)	108.927(94)	108.928(95)	108.928(91)	108.933(87)
$\angle$(O$_8$-C$_3$-C$_4$) / °	128.59(21)	[128.43(17)]	[128.43(18)]	[128.44(17)]	[128.45(16)]
$\angle$(C$_3$-C$_4$-C$_9$) / °	121.49(17)	121.45(13)	121.45(13)	121.45(12)	121.45(12)
$\angle$(C$_3$-C$_4$-C$_5$) / °	107.39(18)	107.199(98)	107.20(1)	107.204(95)	107.214(91)
$\angle$(C$_9$-C$_4$-C$_5$) / °	131.12(20)	[131.35(14)]	[131.36(14)]	[131.34(14)]	[131.34(13)]
$\angle$(C$_4$-C$_5$-C$_1$) / °	108.11(60)	[108.17(25)]	[108.17(26)]	[108.16(25)]	[108.17(24)]
c_a / amu$^{1/2}$ Å	-	0.066(11)	0.065(11)	0.068(11)	0.068(10)
c_b / amu$^{1/2}$ Å	-	0.080(16)	0.079(16)	0.083(16)	0.087(15)
c_c / amu$^{1/2}$ Å	-	0.102(17)	0.101(17)	0.105(16)	0.109(15)
σ / MHz	-	0.040 363	0.041 008	0.039 374	0.037 963

	r_S	M06-2X	B2PLYP	DSD-PBEP86	MP2
d(C$_1$-O$_7$) / Å	1.196(19)	1.193 62(59)	1.193 67(61)	1.193 66(60)	1.193 61(60)
d(C$_1$-O$_2$) / Å	1.390(10)	1.3900(28)	1.3897(29)	1.3896(29)	1.3896(28)
d(C$_3$-O$_2$) / Å	1.3755(32)	1.3721(25)	1.3723(26)	1.3725(25)	1.3724(25)
d(C$_3$-O$_8$) / Å	1.2022(51)	1.2007(1)	1.2006(10)	1.2006(10)	1.2006(10)
d(C$_3$-C$_4$) / Å	1.484 22(29)	1.4853(21)	1.4854(21)	1.4853(21)	1.4852(21)
d(C$_4$-C$_9$) / Å	1.491 99(8)	1.490 16(96)	1.4902(1)	1.490 19(97)	1.490 12(97)
d(C$_4$-C$_5$) / Å	1.327 47(51)	1.3287(29)	1.3298(30)	1.3298(30)	1.3297(30)
d(C$_1$-C$_5$) / Å	1.4920(11)	[1.4847(29)]	[1.4845(30)]	[1.4847(30)]	[1.4846(29)]
$\angle$(O$_7$-C$_1$-O$_2$) / °	122.42(70)	122.28(31)	122.34(32)	122.34(32)	122.34(31)
$\angle$(O$_7$-C$_1$-C$_5$) / °	129.86(75)	[129.86(28)]	[129.78(29)]	[129.78(28)]	[129.79(28)]
$\angle$(C$_5$-C$_1$-O$_2$) / °	107.72(17)	[107.86(10)]	[107.88(10)]	[107.88(10)]	[107.88(10)]
$\angle$(C$_1$-O$_2$-C$_3$) / °	107.82(25)	107.798(86)	107.821(89)	107.819(87)	107.817(86)
$\angle$(O$_2$-C$_3$-O$_8$) / °	122.45(19)	122.61(11)	122.63(11)	122.62(11)	122.61(11)
$\angle$(O$_2$-C$_3$-C$_4$) / °	108.96(20)	108.937(86)	108.930(89)	108.932(87)	108.933(87)
$\angle$(O$_8$-C$_3$-C$_4$) / °	128.59(21)	[128.45(16)]	[128.44(17)]	[128.45(16)]	[128.45(16)]
$\angle$(C$_3$-C$_4$-C$_9$) / °	121.49(17)	121.45(12)	121.45(12)	121.45(12)	121.45(12)
$\angle$(C$_3$-C$_4$-C$_5$) / °	107.39(18)	107.223(90)	107.208(93)	107.210(91)	107.212(91)

$\angle$(C$_9$-C$_4$-C$_5$) / °	131.12(20)	[131.33(13)]	[131.34(14)]	[131.34(13)]	[131.33(13)]
$\angle$(C$_4$-C$_5$-C$_1$) / °	108.11(60)	[108.18(24)]	[108.16(24)]	[108.16(24)]	[108.16(24)]
c_a / amu$^{1/2}$ Å	-	0.070(10)	0.068(11)	0.066(10)	0.068(10)
c_b / amu$^{1/2}$ Å	-	0.090(15)	0.085(15)	0.085(15)	0.088(15)
c_c / amu$^{1/2}$ Å	-	0.113(15)	0.108(16)	0.107(15)	0.111(15)
σ / MHz	-	0.038 339	0.038 61	0.037 486	0.037 296

Tab. S10: Overview of bond distances (d) and angles ($\angle$) obtained with Kraitchman's substitution method (r_S) and mass dependent $r_m^{(2)}$ structure fits where only the underlying computational method is specified of citraconic anhydride (CA). Values in brackets were derived and not fit and the given errors are unreliable σ refers to the uncertainty of the respective structure fit.

	r_S	B3LYP	PBE0	CAM-B3LYP	LC-ωPBE
d(C$_1$-O$_7$) / Å	1.196(19)	1.1892(20)	1.1893(21)	1.1893(19)	1.1897(19)
d(C$_1$-O$_2$) / Å	1.390(10)	1.3866(32)	1.3869(34)	1.3866(31)	1.3870(31)
d(C$_3$-O$_2$) / Å	1.3755(32)	1.3787(34)	1.3784(36)	1.3785(33)	1.3778(33)
d(C$_3$-O$_8$) / Å	1.2022(51)	1.1952(25)	1.1955(27)	1.1953(25)	1.1958(25)
d(C$_3$-C$_4$) / Å	1.484 22(29)	1.4819(26)	1.4821(28)	1.4818(25)	1.4821(26)
d(C$_4$-C$_9$) / Å	1.491 99(8)	1.4840(28)	1.4842(30)	1.4840(27)	1.4845(27)
d(C$_4$-C$_5$) / Å	1.327 47(51)	1.3364(37)	1.3361(39)	1.3361(36)	1.3350(36)
d(C$_1$-C$_5$) / Å	1.4920(11)	1.4790(32)	1.4790(34)	1.48(31)	1.48(32)
$\angle$(O$_7$-C$_1$-O$_2$) / °	122.42(70)	122.20(31)	122.19(32)	122.21(30)	122.19(30)
$\angle$(O$_7$-C$_1$-C$_5$) / °	129.86(75)	129.76(29)	129.78(30)	129.76(28)	129.80(28)
$\angle$(C$_5$-C$_1$-O$_2$) / °	107.72(17)	108.04(12)	108.04(13)	108.03(12)	108.01(12)
$\angle$(C$_1$-O$_2$-C$_3$) / °	107.82(25)	107.818(83)	107.813(88)	107.817(80)	107.808(81)
$\angle$(O$_2$-C$_3$-O$_8$) / °	122.45(19)	122.49(13)	122.49(14)	122.49(12)	122.49(13)
$\angle$(O$_2$-C$_3$-C$_4$) / °	108.96(20)	108.824(93)	108.827(98)	108.827(90)	108.840(91)
$\angle$(O$_8$-C$_3$-C$_4$) / °	128.59(21)	128.69(22)	128.68(23)	128.69(21)	128.67(21)
$\angle$(C$_3$-C$_4$-C$_9$) / °	121.49(17)	121.43(11)	121.43(12)	121.43(11)	121.43(11)
$\angle$(C$_3$-C$_4$-C$_5$) / °	107.39(18)	107.086(96)	107.09(10)	107.094(93)	107.115(94)
$\angle$(C$_9$-C$_4$-C$_5$) / °	131.12(20)	131.49(16)	131.49(17)	131.48(16)	131.46(16)
$\angle$(C$_4$-C$_5$-C$_1$) / °	108.11(60)	108.23(24)	108.24(25)	108.23(23)	108.23(23)
c_a / amu$^{1/2}$ Å	-	0.155(51)	0.151(53)	0.154(49)	0.146(49)
c_b / amu$^{1/2}$ Å	-	0.241(71)	0.236(75)	0.240(69)	0.228(69)
c_c / amu$^{1/2}$ Å	-	0.302(89)	0.297(94)	0.302(86)	0.287(87)
d_a / amu$^{1/2}$ Å^2	-	−0.22(17)	−0.22(17)	−0.22(16)	−0.20(16)
d_b / amu$^{1/2}$ Å^2	-	−0.98(41)	−0.95(43)	−0.96(40)	−0.86(40)
d_c / amu$^{1/2}$ Å^2	-	−1.37(59)	−1.34(62)	−1.34(57)	−1.22(58)
σ / MHz	-	0.042 761	0.044 903	0.041 579	0.041 991
	r_S	M06-2X	B2PLYP	DSD-PBEP86	MP2
d(C$_1$-O$_7$) / Å	1.196(19)	1.1901(20)	1.1894(19)	1.1895(19)	1.1895(19)
d(C$_1$-O$_2$) / Å	1.390(10)	1.3878(33)	1.3867(31)	1.3867(31)	1.3868(31)
d(C$_3$-O$_2$) / Å	1.3755(32)	1.3769(35)	1.3783(33)	1.3781(33)	1.3780(33)
d(C$_3$-O$_8$) / Å	1.2022(51)	1.1965(26)	1.1954(24)	1.1956(24)	1.1956(24)
d(C$_3$-C$_4$) / Å	1.484 22(29)	1.4826(27)	1.4818(25)	1.4819(25)	1.4819(25)
d(C$_4$-C$_9$) / Å	1.491 99(8)	1.4852(29)	1.4841(27)	1.4843(27)	1.4843(27)
d(C$_4$-C$_5$) / Å	1.327 47(51)	1.3335(38)	1.3358(36)	1.3355(36)	1.3353(35)

$d(C_1\text{-}C_5)$ / Å	1.4920(11)	1.4804(33)	1.4794(31)	1.4797(31)	1.4797(31)
$\angle(O_7\text{-}C_1\text{-}O_2)$ / °	122.42(70)	122.15(31)	122.21(29)	122.22(29)	122.21(29)
$\angle(O_7\text{-}C_1\text{-}C_5)$ / °	129.86(75)	129.87(29)	129.77(28)	129.77(28)	129.78(28)
$\angle(C_5\text{-}C_1\text{-}O_2)$ / °	107.72(17)	107.98(12)	108.02(12)	108.02(12)	108.01(12)
$\angle(C_1\text{-}O_2\text{-}C_3)$ / °	107.82(25)	107.792(84)	107.816(80)	107.816(80)	107.814(79)
$\angle(O_2\text{-}C_3\text{-}O_8)$ / °	122.45(19)	122.50(13)	122.49(12)	122.49(12)	122.49(12)
$\angle(O_2\text{-}C_3\text{-}C_4)$ / °	108.96(20)	108.854(95)	108.830(89)	108.835(90)	108.837(89)
$\angle(O_8\text{-}C_3\text{-}C_4)$ / °	128.59(21)	128.64(22)	128.68(21)	128.68(21)	128.67(21)
$\angle(C_3\text{-}C_4\text{-}C_9)$ / °	121.49(17)	121.43(11)	121.43(11)	121.43(11)	121.43(10)
$\angle(C_3\text{-}C_4\text{-}C_5)$ / °	107.39(18)	107.137(98)	107.101(92)	107.107(93)	107.111(92)
$\angle(C_9\text{-}C_4\text{-}C_5)$ / °	131.12(20)	131.44(16)	131.47(16)	131.46(16)	131.46(16)
$\angle(C_4\text{-}C_5\text{-}C_1)$ / °	108.11(60)	108.24(24)	108.23(23)	108.22(23)	108.23(23)
c_a / amu$^{1/2}$ Å	-	0.136(51)	0.153(48)	0.149(49)	0.150(48)
c_b / amu$^{1/2}$ Å	-	0.214(72)	0.238(68)	0.232(68)	0.234(68)
c_c / amu$^{1/2}$ Å	-	0.270(90)	0.299(85)	0.292(86)	0.294(85)
d_a / amu$^{1/2}$ Å^2	-	−0.17(17)	−0.22(16)	−0.22(16)	−0.22(16)
d_b / amu$^{1/2}$ Å^2	-	−0.75(42)	−0.93(39)	−0.90(39)	−0.88(39)
d_c / amu$^{1/2}$ Å^2	-	−1.08(60)	−1.31(57)	−1.26(57)	−1.25(56)
σ / MHz	-	0.043 807	0.041 207	0.041 338	0.041 120

Tab. S11: Overview of bond distances (d) and angles ($\angle$) obtained with Kraitchman's substitution method (r_S) and mass dependent $r_m^{(1)}$ structure fits where only the underlying computational method is specified of itaconic anhydride (IA). σ refers to the uncertainty of the respective structure fit.

	r_S	B3LYP	PBE0	CAM-B3LYP	LC-ωPBE
$d(C_1\text{-}C_5)$ / Å	1.532(17)	1.5081(47)	1.5086(41)	1.5062(49)	1.5073(47)
$d(C_4\text{-}C_5)$ / Å	1.4907(34)	1.5017(77)	1.4991(67)	1.5010(81)	1.4995(76)
$d(C_3\text{-}C_4)$ / Å	1.4789(29)	1.3348(24)	1.3342(21)	1.3337(26)	1.3337(24)
$d(C_4\text{-}C_{10})$ / Å	1.3376(47)	1.4777(70)	1.4789(61)	1.4790(73)	1.4798(70)
$\angle(C_1\text{-}C_5\text{-}C_4)$ / °	102.83(47)	103.22(14)	103.16(12)	103.18(15)	103.15(14)
$\angle(C_5\text{-}C_4\text{-}C_{10})$ / °	130.27(18)	130.42(29)	130.39(26)	130.41(31)	130.41(29)
$\angle(C_5\text{-}C_4\text{-}C_3)$ / °	107.51(17)	107.49(20)	107.39(18)	107.37(21)	107.32(20)
c_a / amu$^{1/2}$ Å	-	0.096(56)	0.112(49)	0.125(59)	0.132(56)
c_b / amu$^{1/2}$ Å	-	0.052(36)	0.114(31)	0.127(38)	0.139(36)
c_c / amu$^{1/2}$ Å	-	0.084(41)	0.144(36)	0.162(43)	0.176(41)
σ / MHz	-	0.080 794	0.096 842	0.117 185	0.122 435
	r_S	M06-2X	B2PLYP	DSD-PBEP86	MP2
$d(C_1\text{-}C_5)$ / Å	1.532(17)	1.5080(48)	1.5105(40)	1.5118(33)	1.5138(30)
$d(C_4\text{-}C_5)$ / Å	1.4907(34)	1.5002(78)	1.5000(65)	1.4985(53)	1.4977(50)
$d(C_3\text{-}C_4)$ / Å	1.4789(29)	1.3337(25)	1.3354(21)	1.3355(17)	1.3362(16)
$d(C_4\text{-}C_{10})$ / Å	1.3376(47)	1.4796(71)	1.4774(59)	1.4780(48)	1.4772(45)
$\angle(C_1\text{-}C_5\text{-}C_4)$ / °	102.83(47)	103.13(14)	103.21(12)	103.177(96)	103.184(89)
$\angle(C_5\text{-}C_4\text{-}C_{10})$ / °	130.27(18)	130.42(30)	130.43(25)	130.41(20)	130.43(19)
$\angle(C_5\text{-}C_4\text{-}C_3)$ / °	107.51(17)	107.32(21)	107.51(17)	107.48(14)	107.53(13)
c_a / amu$^{1/2}$ Å	-	0.141(57)	0.094(47)	0.093(39)	0.089(36)
c_b / amu$^{1/2}$ Å	-	0.129(36)	0.027(30)	0.035(25)	−0.005(23)

c_c / amu$^{1/2}$ Å	-	0.173(42)	0.062(35)	0.069(29)	0.034(26)
σ / MHz	-	0.123 153	0.059 283	0.057 069	0.036 789

Tab. S12: Overview of bond distances (d) and angles ($\angle$) obtained with Kraitchman's substitution method (r_S) and mass dependent $r_m^{(2)}$ structure fits where only the underlying computational method is specified of itaconic anhydride (IA). σ refers to the uncertainty of the respective structure fit.

	r_S	B3LYP	PBE0	CAM-B3LYP	LC-ωPBE
d(C$_1$-C$_5$) / Å	1.532(17)	1.5024(20)	1.5042(10)	1.5007(14)	1.5026(24)
d(C$_4$-C$_5$) / Å	1.4907(34)	1.5075(33)	1.5018(17)	1.5046(23)	1.5017(39)
d(C$_3$-C$_4$) / Å	1.4789(29)	1.3237(18)	1.325 35(95)	1.3229(13)	1.3245(21)
d(C$_4$-C$_{10}$) / Å	1.3376(47)	1.4723(27)	1.4750(14)	1.4742(19)	1.4759(31)
$\angle$(C$_1$-C$_5$-C$_4$) / °	102.83(47)	103.264(55)	103.236(28)	103.268(38)	103.244(64)
$\angle$(C$_5$-C$_4$-C$_{10}$) / °	130.27(18)	130.65(12)	130.654(60)	130.718(81)	130.71(14)
$\angle$(C$_5$-C$_4$-C$_3$) / °	107.51(17)	107.226(82)	107.187(42)	107.117(57)	107.102(96)
c_a / amu$^{1/2}$ Å	-	0.289(48)	0.318(25)	0.371(33)	0.370(56)
c_b / amu$^{1/2}$ Å	-	0.398(62)	0.370(32)	0.445(43)	0.402(73)
c_c / amu$^{1/2}$ Å	-	0.496(58)	0.487(30)	0.579(41)	0.542(68)
d_a / amu$^{1/2}$ Å^2	-	−0.61(20)	−0.75(10)	−0.89(14)	−0.89(24)
d_b / amu$^{1/2}$ Å^2	-	−2.46(46)	−1.77(24)	−2.20(32)	−1.80(54)
d_c / amu$^{1/2}$ Å^2	-	−3.23(46)	−2.65(24)	−3.22(32)	−2.81(54)
σ / MHz	-	0.031 219	0.026 813	0.035 625	0.053 467
	r_S	M06-2X	B2PLYP	DSD-PBEP86	MP2
d(C$_1$-C$_5$) / Å	1.532(17)	1.5030(23)	1.5057(22)	1.5078(13)	1.5103(24)
d(C$_4$-C$_5$) / Å	1.4907(34)	1.5031(39)	1.5055(37)	1.5026(21)	1.5024(40)
d(C$_3$-C$_4$) / Å	1.4789(29)	1.3239(21)	1.3260(20)	1.3277(11)	1.3293(22)
d(C$_4$-C$_{10}$) / Å	1.3376(47)	1.4753(31)	1.4728(30)	1.4743(17)	1.4737(32)
$\angle$(C$_1$-C$_5$-C$_4$) / °	102.83(47)	103.216(63)	103.235(60)	103.210(34)	103.189(64)
$\angle$(C$_5$-C$_4$-C$_{10}$) / °	130.27(18)	130.72(14)	130.59(13)	130.575(72)	130.52(14)
$\angle$(C$_5$-C$_4$-C$_3$) / °	107.51(17)	107.085(95)	107.290(90)	107.293(51)	107.368(97)
c_a / amu$^{1/2}$ Å	-	0.377(56)	0.236(53)	0.226(30)	0.170(56)
c_b / amu$^{1/2}$ Å	-	0.415(72)	0.323(69)	0.276(38)	0.220(73)
c_c / amu$^{1/2}$ Å	-	0.557(67)	0.403(64)	0.358(36)	0.279(68)
d_a / amu$^{1/2}$ Å^2	-	−0.87(23)	−0.42(22)	−0.42(12)	−0.19(24)
d_b / amu$^{1/2}$ Å^2	-	−1.97(53)	−2.12(51)	−1.72(28)	−1.63(54)
d_c / amu$^{1/2}$ Å^2	-	−2.96(53)	−2.70(51)	−2.27(28)	−1.96(54)
σ / MHz	-	0.053 266	0.034 976	0.017 56	0.040 363

4 Computational details and example inputs

Tab. S13: Overview of the different computational method used in this work. The program used, method, basis set, dispersion correction if possible/necessary, functional class for density functionals and type of frequency calculation are given. SCS refers to spin component scaling, VPT2 to vibrational perturbation theory of second order and AE to all electron.

program	method	basis set	dispersion corr.	functional class	frequency
Gaussian 16	B3LYP	aug-cc-pVTZ	D3(BJ)	hybrid	VPT2
Gaussian 16	PBE0	aug-cc-pVTZ	D3(BJ)	hybrid	VPT2
Gaussian 16	CAM-B3LYP	aug-cc-pVTZ	D3(BJ)	range-separated hybrid	VPT2
Gaussian 16	LC-ωPBE	aug-cc-pVTZ	D3(BJ)	range-separated hybrid	VPT2
Gaussian 16	M06-2X	aug-cc-pVTZ	-	meta hybrid	VPT2
Gaussian 16	B2PLYP	aug-cc-pVTZ	D3(BJ)	double hybrid	VPT2
Gaussian 16	DSD-PBEP86	aug-cc-pVTZ	D3(BJ)	SCS double hybrid	VPT2
Gaussian 16	MP2	aug-cc-pVTZ	-	-	VPT2
Molpro 2022	DCSD-F12b	cc-pVDZ-F12	-	-	harmonic
Molpro 2022	CCSD(T)-F12c	cc-pVDZ-F12	-	-	harmonic
Molpro 2022	AE-CCSD(T)-F12c	cc-pVDZ-F12	-	-	harmonic

Tab. S14: Example inputs for the Gaussian 16 (Rev. C.01)[6] calculations at the B3LYP and MP2 level of computation. The `Print` and `Resonances` settings follow one line after the geometry input. Only the method block is shown. Note that the geometry optimisation has been conducted separately from the VPT2 calculation reading the optimised geometry from a checkpoint file. See Tab. S13 whether or not dispersion correction has been applied for a given functional.

calculation	input
optimisation DFT	`# B3LYP aug-cc-pVTZ Int=SuperFine empiricaldispersion=gd3bj output=pickett` `# Opt=VeryTight`
optimisation WFT	`# MP2 aug-cc-pVTZ output=pickett` `# Opt=VeryTight`

VPT2	`# B3LYP aug-cc-pVTZ Int=SuperFine empiricaldispersion=gd3bj output=pickett`
	`# Geom=Checkpoint`
	`# Freq=(anharmonic,ReadAnharm)`
	`Print=(NMOrder=AscNoIrrep)`
	`Resonances=No11Res`

Tab. S15: Example input for the MOLPRO 2022.3[7–9] calculations at CCSD(T) level of theory. Only the method block is shown. For the DCSD-F12b calculations, CCSD(T)-F12c keyword need to be substituted. For all electron (AE) calculations, the `core,0` keyword needs to be added to the CCSD(T)-F12c input line.

```
gthresh,OPTSTEP=6.d-5,OPTGRAD=1.d-6,ENERGY=1.d-12,twoint=1.d-14,ZERO=1.d-16
orient,mass
symmetry,auto
MASS,ISO
geomtyp=xyz
```

```
angstrom
geometry=GEOM_START.xyz
basis=vdz-f12
{HF,accu,16}
{CCSD(T)-F12c,gem_beta=0.9}
{OPTG,GAUSSIAN,GRMS=1.d-5,SRMS=1.d-5}
put,xyz,GEOM.xyz
{frequencies,STEP=0.005
PRINT,HESSIAN,LOW}
```

Literature

[1] A. Kanzow, B. Hartwig, D. A. Obenchain, J.-U. Grabow, *https://doi.org/10.25625/FQCEVB Microwave spectra of Citraconic and Itaconic anhydride*, version V1, GRO.data, **2025**.

[2] A. Kanzow, B. Hartwig, D. A. Obenchain, *https://doi.org/10.25625/IBKABW Computational outputs of DFT, MP2 and Coupled Cluster calculations for geometry optimizations and frequency calculations*, version V1, GRO.data, **2025**.

[3] A. Kanzow, B. Hartwig, D. A. Obenchain, *https://doi.org/10.25625/AFCLSC Experimental XIAM and Pickett Fits, Kraitchman structure and semi-experimental as well as mass dependent structure fits for citraconic and itaconic anhydride*, version V1, GRO.data, **2025**.

[4] N. Vogt, E. P. Altova, N. M. Karasev, "Equilibrium structure of maleic anhydride from gas-phase electron diffraction (GED) and quantum-chemical studies", *Journal of Molecular Structure* **2010**, *978*, ELECTRON DIFFRACTION, THEORETICAL CALCULATIONS, AND MOLECULAR STRUCTURE, 153–157.

[5] M. K. Jahn, D. A. Obenchain, K. P. R. Nair, J.-U. Grabow, N. Vogt, J. Demaison, P. D. Godfrey, D. McNaughton, "The puzzling hyper-fine structure and an accurate equilibrium geometry of succinic anhydride", *Phys. Chem. Chem. Phys.* **2020**, *22*, 5170–5177.

[6] M. J. Frisch, G. W. Trucks, H. B. Schlegel, G. E. Scuseria, M. A. Robb, J. R. Cheeseman, G. Scalmani, V. Barone, G. A. Petersson, H. Nakatsuji, X. Li, M. Caricato, A. V. Marenich, J. Bloino, B. G. Janesko, R. Gomperts, B. Mennucci, H. P. Hratchian, J. V. Ortiz, A. F. Izmaylov, J. L. Sonnenberg, D. Williams-Young, F. Ding, F. Lipparini, F. Egidi, J. Goings, B. Peng, A. Petrone, T. Henderson, D. Ranasinghe, V. G. Zakrzewski, J. Gao, N. Rega, G. Zheng, W. Liang, M. Hada, M. Ehara, K. Toyota, R. Fukuda, J. Hasegawa, M. Ishida, T. Nakajima, Y. Honda, O. Kitao, H. Nakai, T. Vreven, K. Throssell, J. A. Montgomery, Jr., J. E. Peralta, F. Ogliaro, M. J. Bearpark, J. J. Heyd, E. N. Brothers, K. N. Kudin, V. N. Staroverov, T. A. Keith, R. Kobayashi, J. Normand, K. Raghavachari, A. P. Rendell, J. C. Burant, S. S. Iyengar, J. Tomasi, M. Cossi, J. M. Millam, M. Klene, C. Adamo, R. Cammi, J. W. Ochterski, R. L. Martin, K. Morokuma, O. Farkas, J. B. Foresman, D. J. Fox, Gaussian 16 Revision C.01, Gaussian Inc., Wallingford CT, **2016**.

[7] H.-J. Werner, P. J. Knowles, G. Knizia, F. R. Manby, M. Schütz, "Molpro: a general-purpose quantum chemistry program package", *WIREs Comput. Mol. Sci.* **2012**, *2*, 242–253.

[8] H.-J. Werner, P. J. Knowles, F. R. Manby, J. A. Black, K. Doll, A. Heßelmann, D. Kats, A. Köhn, T. Korona, D. A. Kreplin, Q. Ma, T. F. Miller, A. Mitrushchenkov, K. A. Peterson, I. Polyak, G. Rauhut, M. Sibaev, "The Molpro quantum chemistry package", *J. Chem. Phys.* **2020**, *152*, 144107.

[9] H.-J. Werner, P. J. Knowles, P. C. W. Györffy, A. Hesselmann, D. Kats, G. Knizia, A. Köhn, T. Korona, D. Kreplin, R. Lindh, Q. Ma, F. R. Manby, A. Mitrushenkov, G. Rauhut, M. Schütz, K. R. Shamasundar, T. B. Adler, R. D. Amos, J. Baker, S. J. Bennie, A. Bernhardsson, A. Berning, J. A. Black, P. J. Bygrave, R. Cimiraglia, D. L. Cooper, D. Coughtrie, M. J. O. Deegan, A. J. Dobbyn, K. Doll, M. Dornbach, F. Eckert, S. Erfort, E. Goll, C. Hampel, G. Hetzer, J. G. Hill, M. Hodges, T. Hrenar, G. Jansen, C. Köppl, C. Kollmar, S. J. R. Lee, Y. Liu, A. W. Lloyd, R. A. Mata, A. J. May, B. Mussard, S. J. McNicholas, W. Meyer, T. F. M. III, M. E. Mura, A. Nicklass, D. P. O'Neill, P. Palmieri, D. Peng, K. A. Peterson, K. Pflüger, R. Pitzer, I. Polyak, P. Pulay, M. Reiher, J. O. Richardson, J. B. Robinson, B. Schröder, M. Schwilk, T. Shiozaki, M. Sibaev, H. Stoll, A. J. Stone, R. Tarroni, T. Thorsteinsson, J. Toulouse, M. Wang, M. Welborn, B. Ziegler, MOLPRO, version 2022.3, a package of ab initio programs, see https://www.molpro.net, **2022**.